JOURNAL OF GEOPHYSICAL RESEARCH, VOL. 105, NO. A7, PAGES 15,931–15,944, JULY 1, 2000

Cold flowing O^+ beams in the lobe/mantle at Geotail: Does FAST observe the source?

K. Seki,[1,2] R. C. Elphic,[1] M. F. Thomsen,[1] J. Bonnell,[3] E. J. Lund,[4]
M. Hirahara,[5] T. Terasawa,[2] and T. Mukai[6]

Abstract. The Geotail spacecraft observed high-energy (~3-10 keV) cold O^+ beams (COBs) streaming tailward together with protons entering from the magnetosheath in the northern dusk lobe/mantle when the IMF (interplanetary magnetic field) B_y and B_z are steadily negative. He^+ beams were also observed intermittently. During the same period the FAST satellite passed across the dayside northern polar regions from dawn to dusk at low altitudes (1200-3400 km) and observed O^+ precipitation on both closed and open field lines. There are regions where the magnetosheath and dayside plasma sheet/ring current components coexist and are precipitating together. In the open field line regions the precipitating O^+ seem continuous with the precipitation in the closed regions, while the H^+ and He^{++} precipitations are denser and typically have lower energy than O^+. The phase space density (PSD) of the precipitating ions is highly isotropic except for the loss cone in the upward direction. Utilizing Liouville's theorem, we have compared the PSD of locally mirroring O^+ at FAST with the PSD of COBs observed at Geotail. This comparison shows that the PSD in the high-energy precipitation region on closed field lines is comparable to that of the COBs. In regions where the magnetosheath and dayside magnetosphere ions coexist, the O^+ PSD is typically smaller than that of the COBs, but at low latitudes it sometimes reaches values comparable to that of the COBs. These results suggest that the high-energy O^+ ions in the dayside magnetosphere are a promising candidate for the source of COBs in the lobe/mantle. The ion dynamics on reconnected flux tubes needs to be examined further to clarify the possible energization mechanisms and their effect on the O^+ ions.

1. Introduction

Observations of O^+ and He^+ beams in the distant lobe/mantle by Geotail [*Mukai et al.*, 1994a; *Hirahara et al.*, 1996; *Seki et al.*, 1996, 1998a, b, 1999] have shed a new light upon plasma energization and transportation mechanisms in the magnetosphere, since their location up to the largest tailward distances explored by Geotail (~210 R_E) as well as their coexistence with ions of solar wind origin is not explicable with a conventional view of magnetospheric dynamics.

Among the ion species observed in the magnetosphere, O^+ and He^+ are commonly seen in the ionosphere and have been used as indicators of an ionospheric plasma, while He^{++}, which usually makes up a few percent of the solar wind, has been used as an indicator of a plasma of the solar wind origin. From the near-Earth observations [e.g., *Chappell et al.*, 1987; *Yau and André*, 1997, and references therein] it has been suggested that ion outflows from the cusp/cleft regions can contribute significantly to magnetospheric plasmas such as the near-Earth lobe and plasma sheet plasmas, but these ionospheric ions were considered not to be able to reach the distant lobe/mantle, because their outflow energies are usually too low to overcome the magnetospheric convection toward the plasma sheet. In fact, quantitative comparisons of statistical properties of cold O^+ beams (COBs) in the lobe/mantle with those of ionospheric polar O^+ outflows [*Seki et al.*, 1998b] showed the necessity of an extra energization of ~2.7 keV on average so as to supply COBs in the distant tail with polar O^+ outflows. A simulation result by *Delcourt et al.* [1996], which shows a prominent effect of the curvature-related accelerations of O^+ in the enhanced convection, seems to provide a positive suggestion to the extra energization.

On the other hand, the statistical properties of COBs have provided another remarkable clue to the supply mechanisms of these ions of ionospheric origin. Namely, the COBs have

[1]Space and Atmospheric Sciences (NIS-1), Los Alamos National Laboratory, Los Alamos, New Mexico.
[2]Department of Earth and Planetary Sciences, Graduate School of Science, University of Tokyo, Tokyo, Japan.
[3]Space Science Laboratory, University of California Berkeley, California.
[4]Space Science Center, University of New Hampshire, Durham, New Hampshire.
[5]Department of Physics, College of Science, Rikkyo University, Tokyo, Japan.
[6]Institute of Space and Astronautical Science, Kanagawa, Japan.

Paper number 1999JA900470.
0148-0227/00/1999JA900470$09.00

a clear interplanetary magnetic field (IMF) dependence and exist on the "loaded" quadrants of the north-south and dawn-dusk plasma asymmetry where the magnetosheath plasma entry is enhanced through the open flux tubes recently reconnected in dayside. This asymmetry is explicable with IMF B_y effects on the dayside reconnection process and subsequent motion of reconnected flux tubes during southward IMF periods [e.g., *Gosling et al.,* 1985; *Cowley et al.,* 1991, and references therein]. As discussed in detail by *Seki et al.* [1998a] based on properties of COBs, one probable way to explain the clear concentration of COBs on the recently reconnected flux tubes is to consider sources of these ionospheric ions other than the conventional cusp/cleft outflows. One of the candidates of the source of COBs is trapped ions in the subsolar magnetosphere. If a flux tube which contains trapped O^+ ions is reconnected with the IMF at the dayside magnetopause, the O^+ ions will be mixed with the shocked solar wind from the magnetosheath, injected into the high-latitude ionosphere, undergo magnetic mirror reflection, and finally be transported into the tail lobe/mantle, while the flux tube is dragged tailward by the sheath flows. Observations of O^+ and He^+ in the low-latitude boundary layer (LLBL) on recently reconnected field lines [e.g., *Gosling et al.,* 1990; *Fujimoto et al.,* 1997] seem to provide support for this idea.

One of the key issues to investigate the validity of this scenario is whether enough O^+ precipitation exists around the cusp/cleft regions to explain the COB quantitatively or not. As for ion precipitation onto the ionosphere and quantitative identification of various types of dayside precipitation, many studies have been done using polar orbiting satellites [e.g., *Sauvaud et al.,* 1980; *Newell and Meng,* 1988,1992; *Woch and Lundin,* 1992, and references therein]. On the basis of ion and electron precipitation signatures at low altitudes, the dayside ionosphere is classified into several regions such as the cusp, cleft/LLBL, plasma mantle, and ring current/plasma sheet. Among these regions the cusp and plasma mantle are regions where the magnetosheath plasma has direct access to the magnetosphere, and the cleft/LLBL has been attributed to effects of plasma diffusion processes across the magnetopause. It should be noted, however, a recent study suggests that distinction of the cusp and the cleft/LLBL may not be created by different entry processes but simply explained with single process of magnetosheath plasma entry during southward IMF period [*Fuselier et al.,* 1999]. Although the difference between the cusp and cleft/LLBL is not clear and requires future study, observationally, the magnetosheath ions can precipitate in these regions.

On the other hand, the ring current/plasma sheet is considered as a region where equatorially trapped plasma in the magnetosphere exists. From in situ observations near equatorial plane it is well known that the O^+ ions contribute significantly to the ring current/plasma sheet plasma especially at geomagnetically active times [e.g., *Young et al.,* 1982; *Stokholm et al.,* 1989]. This naturally suggests an O^+ contribution to the ion precipitation onto the low-latitude ionosphere. However, most of the previous studies on ion precipitation are about protons and there seems no report about the quantitative properties of O^+ precipitation on either closed or open flux tubes for the energy range of interest ($\leq$20 keV). This may be because of the high time resolution and sensitivity required for its detection, since the flux of the O^+ precipitation can be by a few orders of magnitude less than that of H^+.

Utilizing the high-quality data from the FAST satellite which provides excellent time resolution and sensitivity, we have investigated the properties of O^+ precipitation onto the dayside ionosphere during the COB event on April 7-8, 1998, when the Geotail spacecraft observed high-energy (3-10 keV) COBs in the northern dusk plasma mantle. During this event, solar wind speed and density were almost constant and IMF B_y and B_z were steadily negative. In order to investigate the above issue of the plasma supply process to the magnetotail, i.e., whether the equatorially trapped O^+ ions can be a source of high-energy COBs in the lobe/mantle regions or not, we compare the phase space density (PSD) of precipitating O^+ ions around the cusp with that of COBs in the magnetotail using Liouville's theorem, which ensures to "map" PSDs by considering particle motion and has been used to compare the distribution function of plasmas in different regions [e.g., *Curran and Goertz,* 1989; *Chen et al.,* 1994] The result suggests the importance of equatorially trapped O^+ ions as a potential candidate of the O^+ beams in the lobe/mantle regions.

2. Instrumentation

The Geotail spacecraft was launched on July 24, 1992. Its scientific objective is to study the structure and dynamics of the Earth's magnetotail. The top five panels in Plate 1 show the magnetic field (MGF) and low-energy particle (LEP) observations by Geotail on April 7 and 8, 1998. For technical details about the MGF and LEP instruments onboard Geotail, we refer readers to the literature [*Kokubun et al.,* 1994; *Mukai et al.,* 1994b]. The energy range of energy-per-charge analyzer for ions (EA-i), a part of the LEP instrument, is 32 eV/q to 39 keV/q. There are two data acquisition modes in the LEP. In the 3-D mode, fully 3-D distribution functions $f(v)$ are obtained for 8 hours a day on average. In the 2-D mode, 2-D quasi-equatorial projections of the original $f(v)$ and their onboard 3-D moments (density, velocity, and pressure tensor) are obtained with a full time coverage. In the time period of interest in this paper, Geotail only has the 2-D mode data sets. The MGF instrument provides the 3-D magnetic field data. Both the plasma and magnetic field data used here have a time resolution of 12 s.

The FAST (Fast Auroral Snapshot) satellite was launched into a 4180×350 km, 82.9-deg inclination orbit on August 21, 1996. Its aim is to investigate plasma processes occurring in the low-altitude auroral acceleration region [*Carlson et al.,* 1998]. With this aim, instruments onboard FAST are designed to provide good temporal and spatial resolution data both of particles and fields in polar regions. The FAST plasma instrumentation includes the time-of-flight energy angle mass spectrometer (TEAMS) as well as electrostatic analyzers (ESA) for electrons and ions. The ESA in-

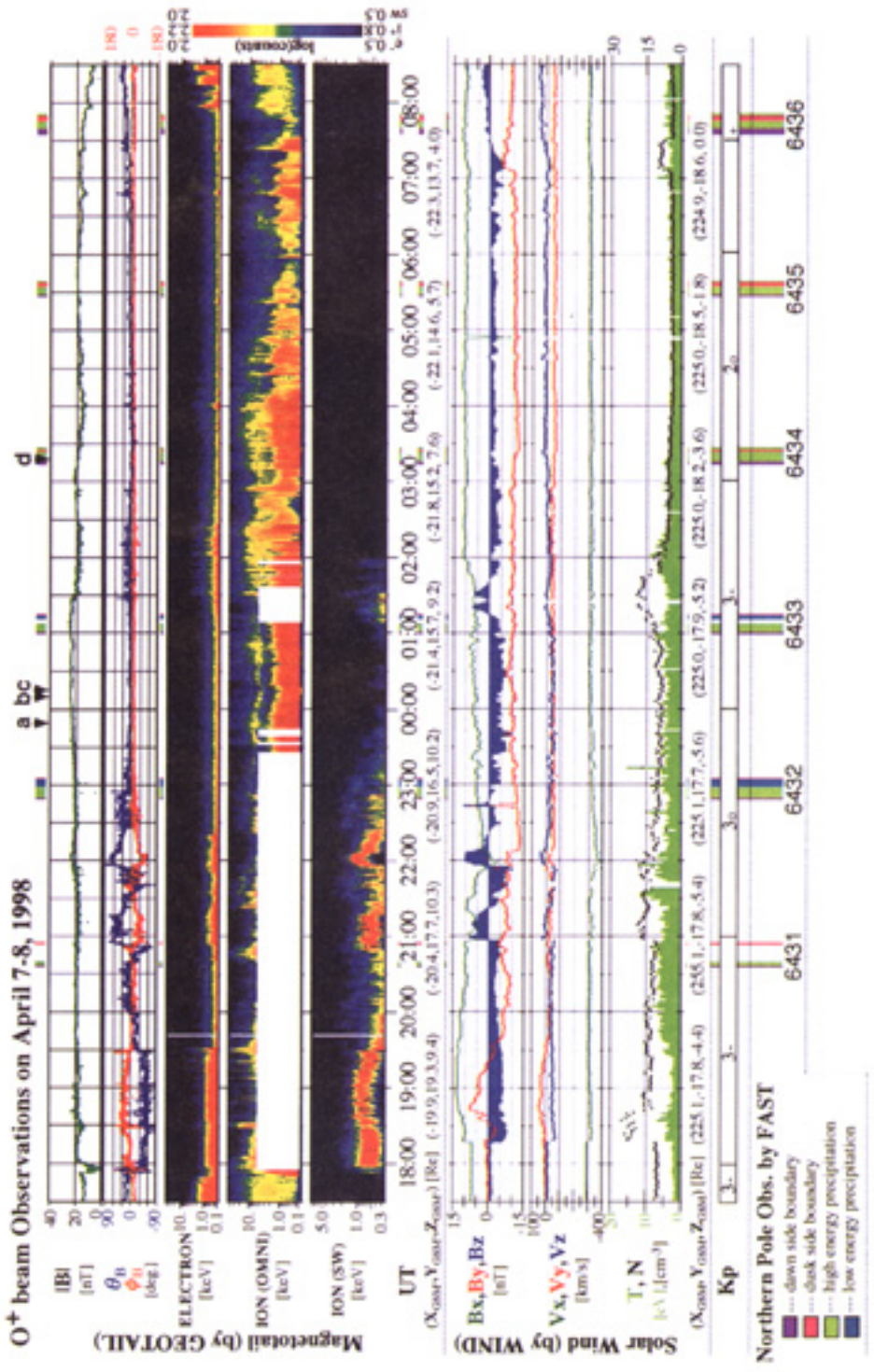

Plate 1. Summary plots of Geotail, Wind, and FAST observations for the O^+ beam event on April 7-8, 1998. From the top, the first two panels display the magnetic field observed by Geotail as magnitude $|\mathbf{B}|$, elevation θ_B from the X_{GSM}-Y_{GSM} plane, and azimuth ϕ_B from the X_{GSM} axis. The next three panels just below them show the energy-time spectrograms for omnidirectional electrons and ions, and ions by the solar wind sensor which only observes strong antisunward flows. Below the time axis, Geotail location in GSM coordinates are displayed. Interplanetary magnetic field, solar wind velocity, density, and temperature observed by Wind are shown in the bottom three panels whose time axis is shifted behind by 83.7 min to correct for the travel time between Geotail and Wind. The coordinate system used in this plate is the GSM. Below these three panels of solar wind conditions, the location of Wind in GSM and simultaneous *Kp* indices are presented. The numbers and color bars at the bottom of the plate show the orbit number of FAST and time intervals when FAST observed the northern polar magnetosphere, respectively. Different colors correspond to different ion precipitation signatures as explained in the bottom left corner of the plate.

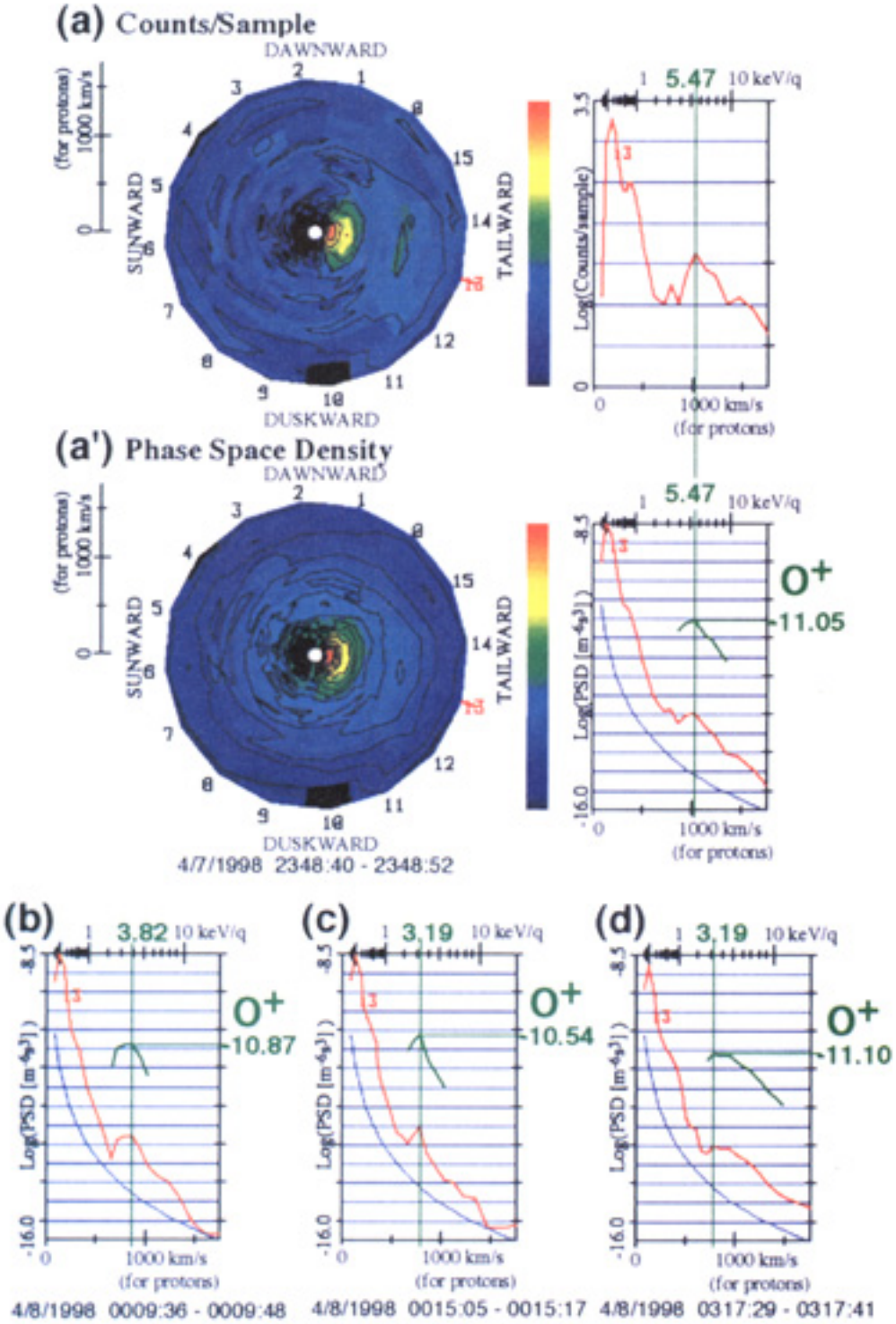

Plate 2. Examples of the ion distributions of the multicomposition ion flows observed by Geotail in the velocity space. Plates 2a-2d correspond to time periods indicated by black arrows at the top of Plate 1. The right panels of Plate 2a and 2a' display projections of counts/sample and phase space density (PSD) onto the equatorial plane for the same interval. Their right pancls and Plate 2b and 2d are cross sections along the azimuthal sector 13 which is the closest to the peak of multicomposition ion flows. The red lines in the right panel of Plate 2a' and Plates 2b-2c display the PSDs calculated assuming the all ions as protons. Thc grcen lines above them are drawn assuming that thc ions are O^+ for high-energy component.

struments measure full pitch angle distributions of electrons (3 eV to 25 keV) and ions (4 eV to 30 keV) and its best time resolution is 78 ms [*Carlson and McFadden,* 1998]. The TEAMS instrument can determine the energy, mass per charge, and incoming direction of ions over energy range of 1 eV to 12 keV and measure 3-D distribution of each ion species with time resolution up to 1/2 spacecraft spin (~2.5 s) [*Möbius et al.,* 1998]. If there is an intense flux of H^+, there can be some contamination to higher m/q bins in TEAMS. All data points in which this problem occurs are excluded from the analysis.

During the time interval of the event reported in this paper, the TEAMS has trouble with onboard data accumulation and the pitch angle distributions at certain energies are not reliable. (It does not cause any problem with the omnidirectional energy-time spectrogram.) In order to remove the problem, we have corrected TEAMS data assuming that the four major ion species (H^+, He^{++}, He^+ and O^+) have the same pitch angle distribution as that observed by the ion electrostatic analyzer (IESA) at each energy bin. After the correction of TEAMS counts at every energy bin under this assumption, the energy flux ratio of each ion species observed by TEAMS is multiplied to the energy flux by IESA at correspondent energy bin to calculate the phase space density (PSD) and moments of H^+, He^{++}, He^+ and O^+. The possible error due to this data accumulation problem is estimated from difference between PSDs calculated with and without the data correction. The error corresponds to ~14% of calculated PSD values on average at highest energy used in this paper (5.467 keV) and decreases in lower energies. As shown afterward, these errors do not affect the conclusion of this paper.

3. Observations

3.1. Magnetotail Observation by Geotail and Solar Wind Conditions

The Geotail spacecraft observed tailward flowing cold O^+ beams in the northern-dusk plasma mantle of the Earth's magnetotail on April 7-8, 1998. Plate 1 shows the outline of the event. The top five panels show the observations by Geotail: From the top, the first two panels display the magnetic field strength and orientation, and the next three panels show the energy-time (*E-t*) spectrograms for omnidirectional electrons, ions, and ions by the solar wind sensor which is less sensitive than the other two and observes only a limited angle range around the sunward direction. As shown just below the time axis, Geotail was located about X_{GSM} ~-21 R_E and goes into the magnetotail from northern-dusk (Y_{GSM} varies from ~20 to ~13.5 R_E).

The bottom three panels of Plate 1 present solar wind conditions observed by Wind during the same period. Their time axis is shifted to the right by 83.7 min, to account for the distance between Geotail and Wind as well as the average solar wind speed (V_x ≈-312.1 km/s) which is very steady during the period of interest as shown by green line in the second bottom panel. The red line in the third panel from the bottom shows that the interplanetary magnetic field (IMF) B_y is steadily negative from 1920 UT on April 7 to 0730 UT on April 8, and simultaneously IMF B_z is almost southward except for time intervals of 2057-2123, 2156-2216, 2243-2246, and 0115-0142 UT as shown by the blue bar graph.

After 1800 UT, Geotail was first in the magnetosheath as indicated by significant tailward ion counts in the ion(SW) *E-t* (the fifth panel from the top). From 1930 UT, Geotail began to skim the mantle-like boundary layer and finally went into the magnetosphere. Comparison of IMF B_z (blue bar graph of Plate 1) with tailward ion counts in the ion(SW) *E-t* (the fifth panel from the top) suggests that Geotail, without exception, went back to the magnetosheath with these northward turnings of IMF. During the negative IMF B_y period (after 1920 UT on April 7), the northern-dusk quadrant of the magnetotail, where Geotail was located, corresponds to one of the loaded quadrants of the tail plasma asymmetry caused by motion of reconnected flux tubes at the dayside magnetopause [e.g., *Gosling et al.,* 1985]. Thus the relocations of Geotail to the magnetosheath during northward IMF periods seem to be due to the interruptions of energy supply from reconnected flux tubes and consequent reduction of the magnetotail volume. This feature also suggests that the time adjustment between Wind and Geotail is reasonable.

Now, let us look at the Geotail data in more detail. As shown in the *E-t*s of OMNI and SW ions, Geotail observed multiple ion flows at different energies in the mantle region. For example, from 2225 to 2310 UT, SW instrument observed two distinct ion flows at different energies of ≤0.5 keV and 0.8-2 keV and the EAi (ion OMNI Et) detected one more ion component at high energy of 5-10 keV. This three-population ion flow continues intermittently to 730UT. Plate 2 shows examples of the counts/sample or the phase space density (PSD) of the multicomposition ion flows observed by Geotail at the time periods indicated by black arrows at the top of Plate 1. As shown in the left panels of Plate 2a and 2a', these ions are streaming tailward. Their right panels show that counts/sample has three peaks at energies of 0.16, 0.76, and 5.47 keV, respectively. From the ratio of energy perpendicular to the local magnetic field (0.23:1:4.5), these three components at the low, middle and high energy are most likely to consist of H^+, He^+, and O^+ ions, since the perpendicular velocity in the lobe/mantle primarily comes from **ExB** drift and tail flapping, and is independent of the particle mass and charge state. This same method of the ion species identification has been used before [e.g., *Seki et al.,* 1999, and references therein].

The red lines in the right panel of Plate 2a' and Plates 2b and 2c display the PSDs calculated under the assumption that the all ions are protons. Owing to the sensor design, if the highest energy ion component is O^+, the PSD should be multiplied by 16^2 and the derived PSDs of O^+ are shown by the green line in each plate. As shown, the PSD at the peak energy of O^+ beams are the order of 10^{-11} $m^{-6}s^3$. Their PSD will be compared later with that observed by FAST.

3.2. Low-Altitude Northern Polar Magnetosphere Observations by FAST

As shown by color bars at the bottom of Plate 1, FAST crossed the dayside northern pole from dawn to dusk six

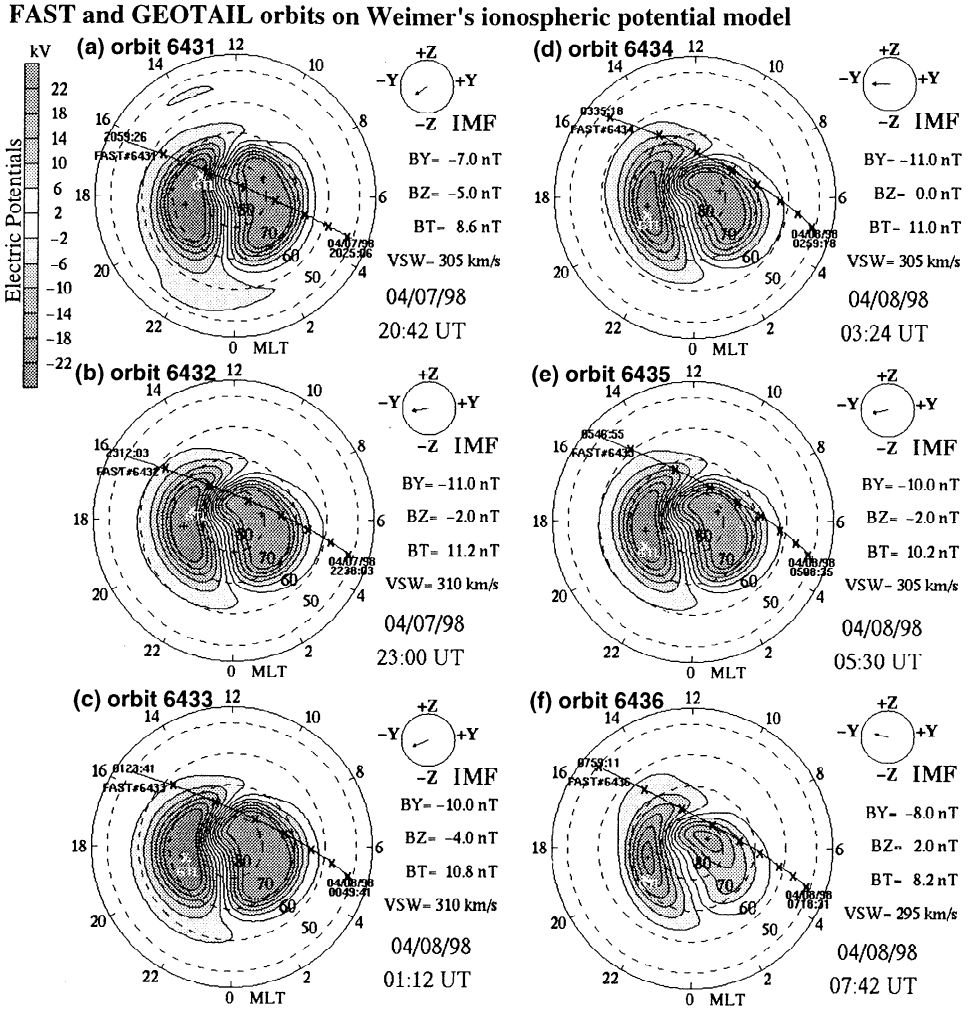

Figure 1. Foot points of the FAST orbit (black crosses) are shown together with the ionospheric electric potential (solid contours) estimated from *Weimer*'s [1996] model under IMF conditions at the center-time of the orbit as shown in the righthand side of each panel. Figures 1a-1f corresponds to orbits 6431-6436, respectively. In each figure, the duskside potential cell (left-hand side) has negative values of the electric potential. The white cross marks display the foot-point of the Geotail orbit at the time shown in the righthand side.

times during this event. Figure 1 displays the foot points of these 6 FAST orbits together with the ionospheric electric potential estimated by Weimer's model [*Weimer,* 1995, 1996] under IMF conditions at the middle of the orbit. The foot point of the Geotail orbit at the same time is also displayed in Figure 1 by white cross marks. It should be noted, however, that the effective Geotail foot point may be shifted towards dayside by the convection, since the ion travel time from FAST to Geotail is ~11 min for 4 keV O^+. As shown by black lines and cross marks, FAST was located in the polar cap but far from the cusp in orbit 6431 and getting closer to the cusp in later orbits.

Plates 3a-3e show the particle observation by FAST/ESA in orbits 6431, 6432, 6433, 6434, and 6436, respectively. The black arrows at the bottom indicate the timing when the FAST passed across the zero potential of Weimer's model. From the top of each plate, energy-time (*E-t*) spectrograms for electrons and ions, and the pitch angle distribution for ions above 80 eV are displayed. As for orbit 6435, which we will see in detail later, the same format of data is shown in the top three panels of Plate 4a. Ram ions due to the satellite motion, which are sometimes accelerated by negative satellite potential and can have energy larger than "ram energy," are responsible for the intense, low-energy fluxes in the ion *E-t* spectrograms. We will ignore these ions and focus on the high-energy ions above 80 eV in subsequent discussions.

As expected from orbit shown in Figure 1, FAST observed a well developed polar cap in orbit 6431 from 2041:20 to 2052:45 UT between the high energy precipitation. The polar cap is also observed in orbit 6433 from 0107:15 to 0110:15 UT. Outside the polar cap, we observed ion precipitation which has a single loss cone in the upward direction (pitch angle around 180°). This is shown in Plates 4b-4e, which display the energy flux distributions above 80 eV corresponding to time intervals indicated by the red arrows at the top of Plate 4a. The antifield direction is to the left in each plate. No upgoing ions are observed within the loss cone and the variation in the width of the loss cone with the altitude of FAST suggests that these ions either are precipitating or have mirrored at lower altitudes.

A remarkable point is that the single loss-cone ion precipitation can be classified into two groups. For example, in orbit 6432 shown in Plate 3b the ion precipitation from 2248:50 UT to 2256:40 UT is accompanied by high-energy electron precipitation. It is most likely on closed flux tubes and is due to the trapped ions in the dayside plasma sheet, since electrons are usually considered to have too large velocity to remain on open flux tubes. However, it is not easy to distinguish open/closed regions only from the electron data, since there often exist electrons accelerated by a parallel potential drop in an energy range similar to that of plasma sheet electrons. One useful method to distinguish open/closed regions is to look at the He^{++} flux. For example, the downgoing flux of He^{++} increases by about one order of magnitude from 2256:40 to 2303:20 UT (not shown), which suggests a significant contribution of magnetosheath plasma to the ion precipitation during this period. The dispersed energy signature of the ions during this interval is consistent with the latitude dependence of precipitating ion energy in the cusp. Thus there are two contributors to the single loss-cone ion precipitation, i.e., the dayside plasma sheet (DPS) and magnetosheath (MS).

In the later orbits 6434-6436 it is difficult to distinguish the MS-originated and DPS-originated precipitation. The time intervals of MS-precipitation in each orbit, inferred from increase of He^{++} flux, are 0320:00-0325:30 UT, 0534:35-0537:35, and 0745:45-0749:15 UT, respectively. During these intervals we can see the coexistence of intense relatively low energy ions and a high-energy component which seems continuous with the high-energy DPS-precipitation on the closed flux tubes. This behavior becomes clearer when we look at the observations of different ion species. The bottom four panels of Plate 4a show the *E-t* spectrograms for different ion species (H^+, He^{++}, He^+ and O^+) observed by the mass-spectrometer (TEAMS) on orbit 6435. It should be noted that ~10 % of the He^{++} counts may be contamination from H^+, while the contamination of He^+ and O^+ by H^+ is negligible.

During the interval of DPS-ion precipitation on closed flux tubes from 0527:55 to 0534:35 UT and after 0537:35 UT, a significant contribution of O^+ is seen. Its intensity decreases, but the O^+ component continues into the region of open flux tubes (0534:35-0537:35 UT). On the other hand, the intensity of He^{++} and H^+ precipitation is enhanced on these open flux tubes. As shown in Plates 4d and 4e, both the high-energy DPS-like precipitation and the intense relatively low-energy MS-like precipitation exist on the same flux tubes. A similar feature can also be seen near the zero-potential time (black arrows in Plate 3) in orbits 6434 and 6436. These results suggest that the DPS plasma of terrestrial origin and the MS plasma of solar wind origin sometimes coexist on the recently reconnected flux tubes in the cusp near the dayside open-closed boundary.

3.3. PSD Comparison

Observations by FAST in the previous subsection reveal that high-energy O^+ ions are precipitating over a wide range of the dayside polar ionosphere, and sometimes they can exist even on open flux tubes. The high-energy O^+ ions precipitating on the reconnected flux tubes at the dayside magnetopause undergo magnetic mirror reflection and some of them might reach the plasma mantle and lobe regions of the magnetotail where Geotail is located during this particular event. In this subsection we will compare the Geotail and FAST observations quantitatively in order to investigate the validity of trapped O^+ ions in the dayside magnetosphere as a source of high-energy O^+ beams in the lobe/mantle.

Since some precipitating particles have reflected before they reach the low altitudes where FAST is located, the upgoing flux is not the appropriate quantity to compare these observations at two different locations. One possible way to compare them quantitatively is to compare the phase space density (PSD) at the two locations utilizing Liouville's theorem. Figure 2 illustrates PSDs of O^+ observed by FAST (Figure 2a) and Geotail (Figure 2b), respectively. Now let us direct our attention to ions at typical O^+ beam energy in the magnetotail and assume that no extra energization occurs between FAST and Geotail locations. When we trace the PSD of O^+ ions whose pitch angle at FAST θ_F is 90 deg (solid circles in Figure 2a) to the Geotail position in the plasma mantle, it will move along a constant-energy surface, reducing its pitch angle to θ_G which satisfies $\sin^2\theta_G = B_G/B_F$ (solid circles in Figure 2b) because of the change in magnetic field strength. Utilizing this feature, we have compared PSDs observed by FAST and Geotail. Practically, the θ_G obtained from the difference of the magnetic field strength between Geotail and FAST is typically a few degrees and much less than the angular resolution of the Geotail instrument. Thus the PSD of O^+ mirrored at FAST moves into an angular bin including the peak PSD of O^+ beams at Geotail, and we compare these two PSDs.

Plate 5b shows the O^+ PSD at energies of 3.188 (orange) and 5.467 (red) keV as well as H^+ PSD at energies of 163 (dark blue) and 487 (light blue) eV observed by Geotail. As shown in the *E-t* spectrogram for ions during the same interval (Plate 5a), the typical energy of O^+ beams is 3-6 keV. Orange and red circles in Plate 5b show that the peak PSD

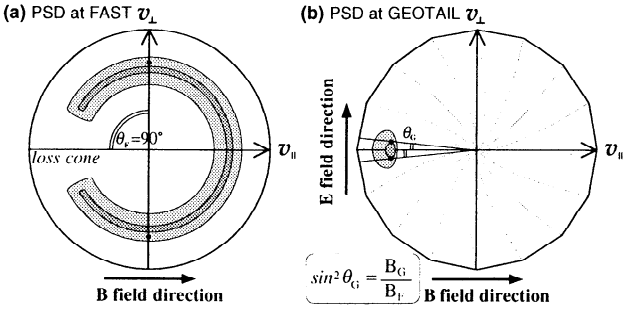

Figure 2. The idea of the PSD comparison between FAST and Geotail is illustrated schematically. The contours in left and right panels show the O^+ phase space density (PSD) observed (a) in low-latitude polar magnetosphere and that (b) in the plasma mantle, respectively. The solid circles indicate the points where the PSDs are compared based on Liouville's theorem, reflecting a change in the pitch angle due to difference of the magnetic field strength between two regions.

of O^+ beams is almost constant in time and of the order of 10^{-12} or 10^{-11} $m^{-6}s^3$. This value does not change significantly in later time periods and the average O^+ PSDs at 3.188 and 5.467 keV are 3.02×10^{-12} and 1.54×10^{-12} $m^{-6}s^3$, respectively.

Next, we compare these values with the PSD at pitch angles of 90° observed by FAST. Plate 6 shows the PSD of H^+ (dark and light blue diamonds) and O^+ (orange and red circles) observed by FAST at the same energies as those displayed in Plate 5b. From the top of Plate 6, each panel corresponds to a different orbit as shown in the top right corner. The horizontal orange and red lines display the average O^+ PSD observed by Geotail at energies of 3.188 and 5.467 keV, respectively. The time interval indicated by a green bar at the bottom of each panel corresponds to the open flux tube regions where the downward He^{++} flux is enhanced or clear polar cap features are observed. As mentioned in the instrumentation section, these PSDs can contain errors due to a problem of onboard data accumulation, and mean error levels for 0.163 keV H^+ (dark-blue), 0.487 keV H^+ (light-blue), 3.188 keV O^+ (orange), and 5.467 keV O^+ (red) correspond to ~1, ~2, ~12, and ~14 % of displayed PSD values, respectively. These errors are small enough for the following comparison with Geotail observations.

In the first three orbits, 6431-6433, there are no significant O^+ counts at the energies of interest on open flux tubes. However, as observed in such intervals as 2035:30-2037:45, 2248:40-2254:10, 0059:30-0105:35, 0313:00-0315:10, and 0739:45-0743:30 UT, the PSDs of precipitating dayside plasma sheet O^+ on closed flux tubes is comparable to that of O^+ beams in the magnetotail. Another remarkable feature is that even on the open flux tubes, there exists high-energy O^+ precipitation as in orbits 6434-6436, and that the PSD of this high-energy O^+ is typically less than that of O^+ beams in the magnetotail but is sometimes at comparable values. These results suggest the importance of equatorially trapped high energy O^+ ions as a potential candidate of the O^+ beams in the lobe/mantle regions.

4. Summary and Discussions

From 2130 UT on April 7 to 0735 UT on April 8, 1998, the Geotail spacecraft observed high-energy (~3-10 keV) cold O^+ beams (COBs) flowing tailward together with He^+ and H^+ in the northern dusk plasma mantle at X_{GSM} ~-21 R_E. During the interval the interplanetary magnetic field (IMF) B_y and B_z were almost steadily negative, and the FAST satellite passed across the dayside northern polar region from dawn to dusk six times at altitudes of 1200-3400 km, observing several types of ion precipitation.

Ion precipitation observed by FAST in a wide range of MLT and ILAT of the dayside polar magnetosphere typically has an isotropic distribution except for a loss cone in the upward direction and sometimes contains heavy ions such as He^{++} He^+ and O^+ in addition to the major H^+ component. This ion precipitation with a single loss cone can be roughly classified into two groups. One is the high-energy ion precipitation in the relatively low latitude and flanks in which the O^+ contribution is significant, and the other is the intense cusp-type precipitation sometimes with dispersed-energy signature and in which the He^{++} flux increases. A remarkable point is that these two types of ion precipitation coexist in the orbits skimming near the dayside separatrix around the cusp. In other words, there exist flux tubes which contain plasma of both magnetosheath and dayside plasma sheet (or low-energy tail of the ring current) origin. Such a mixture is expected in the LLBL. These observations confirm the existence of O^+ precipitation in the cusp which have been potentially expected by previous O^+ observations in the dayside magnetosphere [e.g., *Stokholm et al.,* 1989; *Gosling et al.,* 1990; *Fuselier et al.,* 1991] but had not yet been confirmed.

The COB energy observed by Geotail in the tail plasma mantle is in a range from 3 to 10 keV. This energy is much higher than the typical energy of cusp/cleft originating ions which are traditionally considered to feed the near-Earth lobe plasma [e.g., *Chappell et al.,* 1987], and the investigation of energization and supply mechanisms of these high-energy COBs has been one of the outstanding problems in the magnetospheric physics [e.g., *Hirahara et al.,* 1996, 1998; *Seki et al.,* 1998a, b, 1999]. On the basis of statistical properties of COBs in the lobe/mantle regions observed over a wide range of distances up to $X_{GSM} = -210\ R_E$, *Seki et al.* [1998a] have discussed possible supply scenarios of these high-energy COBs to the magnetotail and came to the conclusion that there seem to be three surviving candidates (see Figure 6 of *Seki et al.* [1998a]). Other than extra energizations of cusp/cleft originating ions, two possible supply mechanisms of COBs are proposed. One of the candidates is to consider the trapped O^+ ions in the closed flux tubes in the dayside magnetosphere as a source of COBs in the magnetotail as illustrated in Figure 3. Once the Earth's magnetic field is reconnected with the IMF at the dayside magnetopause, equatorially trapped O^+ bouncing along the field line will now be on open flux tubes. Some O^+ ions on the newly-reconnected flux tubes will continue to precipitate into the high-latitude ionosphere and undergo magnetic mirror reflection without experiencing energization around the reconnection site. There will be also some O^+ ions which mix with magnetosheath ions from the opposite side, get energized around the reconnection site [*Sonnerup,* 1984, and references therein], then be injected into the high-latitude ionosphere and mirrored, and finally be transported into the tail lobe/mantle, as the reconnected flux tube is dragged tailward. In this event, FAST is observing a part of the injected O^+ ions into the dayside high-latitude ionosphere. Thus we can investigate the validity of the scenario by comparing O^+ observations in the two different regions observed by Geotail and FAST.

We have compared phase space densities (PSDs) of O^+ at typical COB energies utilizing Liouville's theorem. The results can be summarized as follows:

1. In the high-latitude energy-dispersion regions, there is no O^+ precipitation which has energies comparable to those of COBs in the plasma mantle.

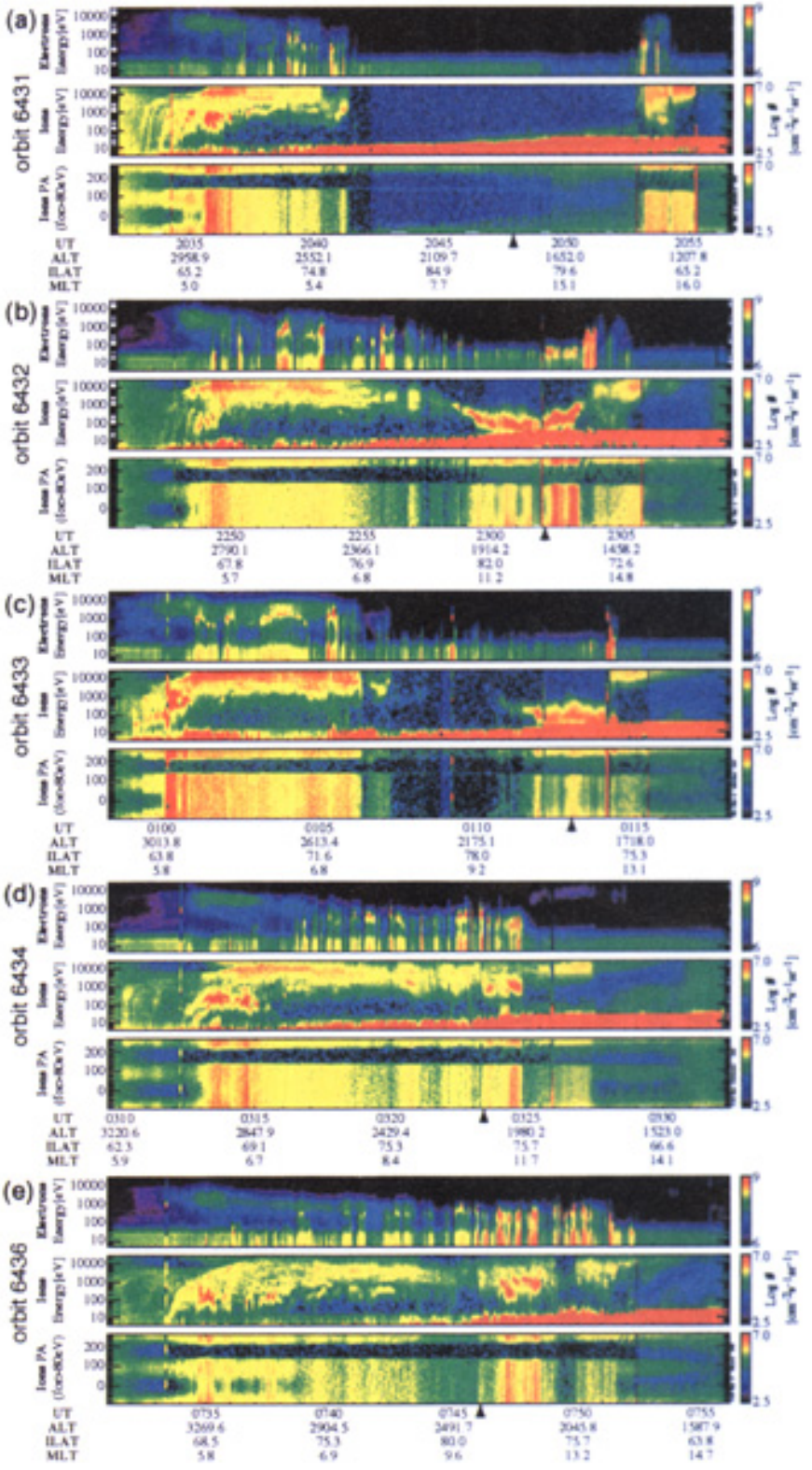

Plate 3. Particle observations by FAST/ESA during the northern polar magnetosphere passages in orbits (a) 6431, (b) 6432, (c) 6433, (d) 6434, and (e) 6436. The black arrows at the bottom of each plate indicate the time when the FAST passed across the zero electric potential inferred from Weimer's model. From the top, each plate shows the energy-time (*E-t*) spectrograms for electrons and ions, and the pitch angle distribution for ions above 80 eV. At the bottom of the plates, the universal time (UT), altitude (ALT), invariant latitude (ILAT), and magnetic local time (MLT) are displayed.

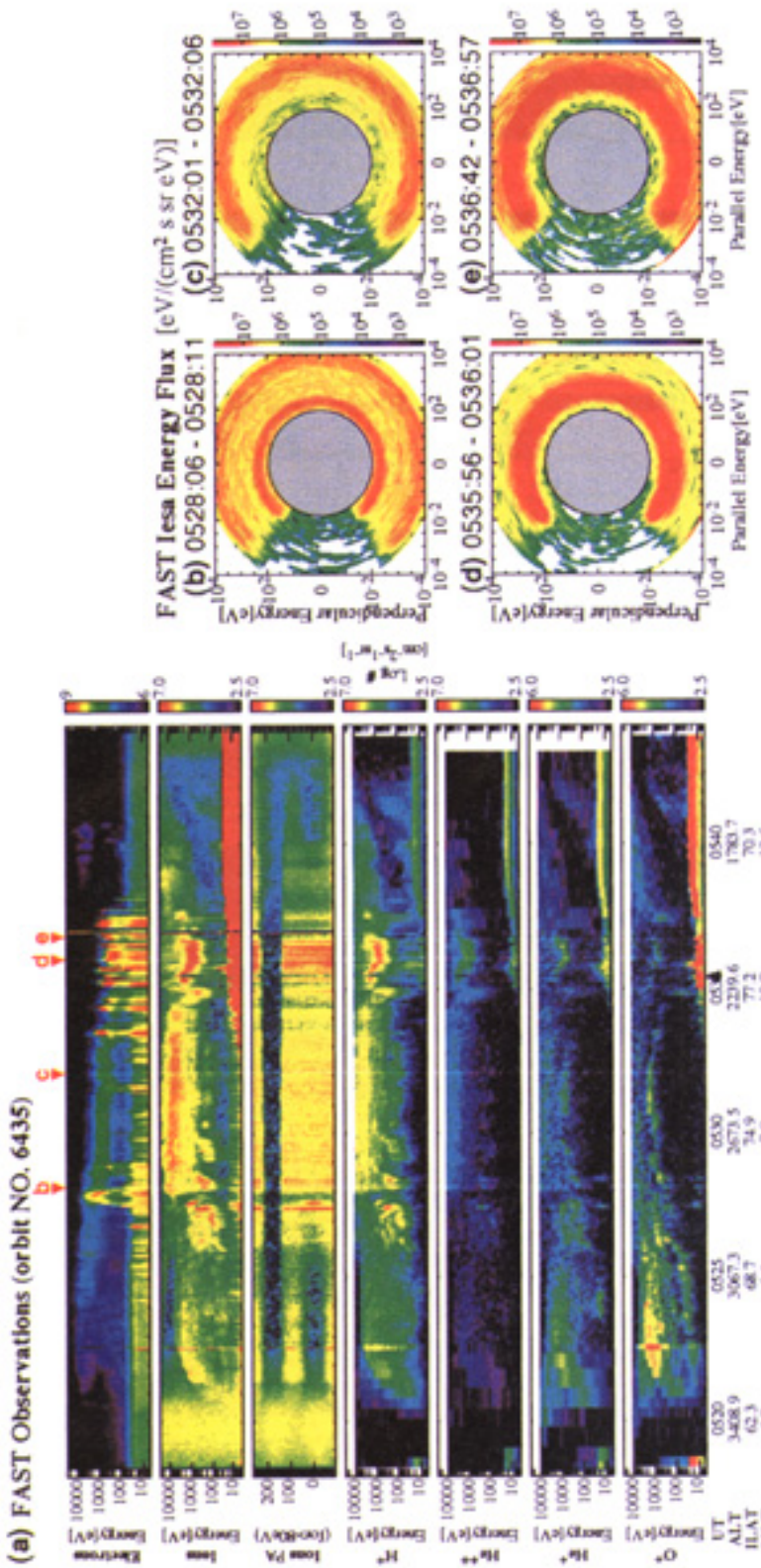

Plate 4. Low-altitude northern pole observations by FAST in orbit 6435. The top three panels of Plate 4a display the *E-t* spectrograms for electrons and ions, and the pitch angle distribution for ions above 80 eV, respectively, observed by electrostatic analyzer (ESA). The bottom four panels show the *E-ts* for different ion species (H^+, He^{++}, He^+, and O^+ from the top) observed by the mass-spectrometer (TEAMS) during the same interval. Energy flux distributions above 80 eV corresponding to the time intervals indicated by red arrows at the top of Plate 4a are displayed in Plate 4b-4e. At the bottom of the plates, the zero-potential crossing, the universal time (UT), altitude (ALT), invariant latitude (ILAT), and magnetic local time (MLT) are indicated in the same format as Plate 3.

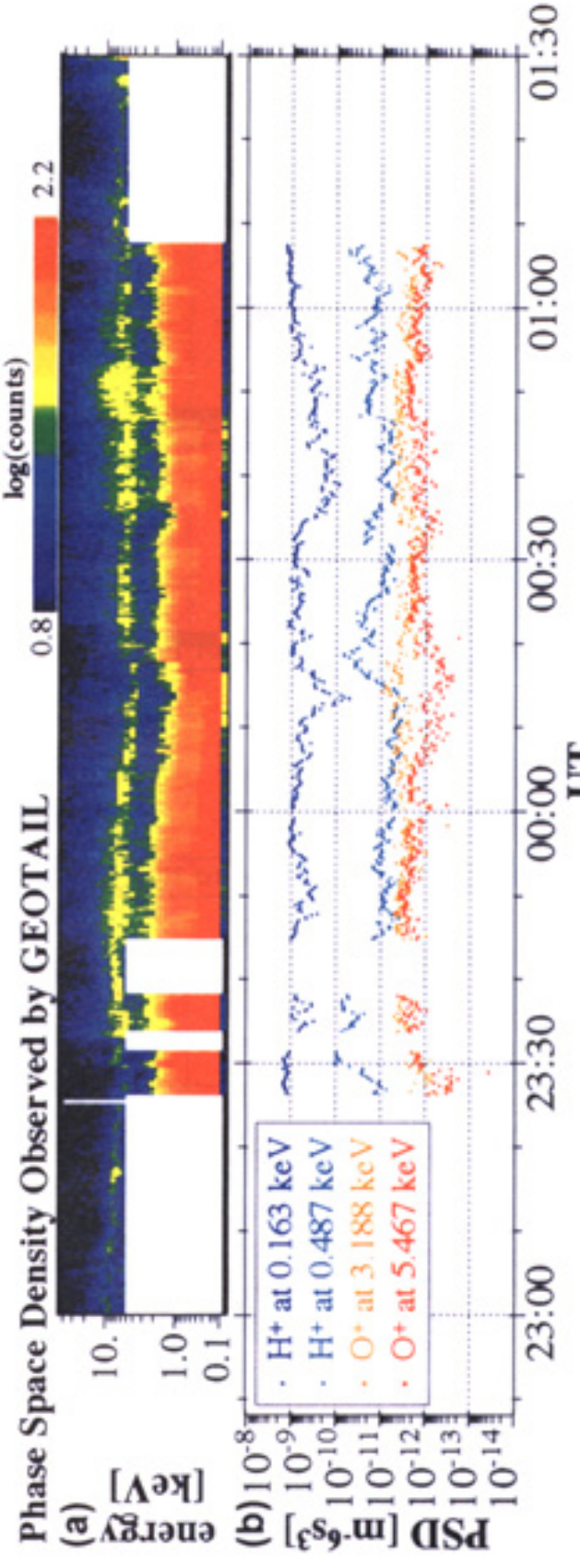

Plate 5. Phase space density (PSD) observed by Geotail. The red, and orange circles in the bottom panel display the O^+ PSDs at energies of 3.188 and 5.467 keV, respectively. The light and dark blue diamonds correspond to the H^+ PSDs at energies of 163 and 487 eV. For reference, the *E-t* spectrogram for ions during the same interval is shown at the top of the plate.

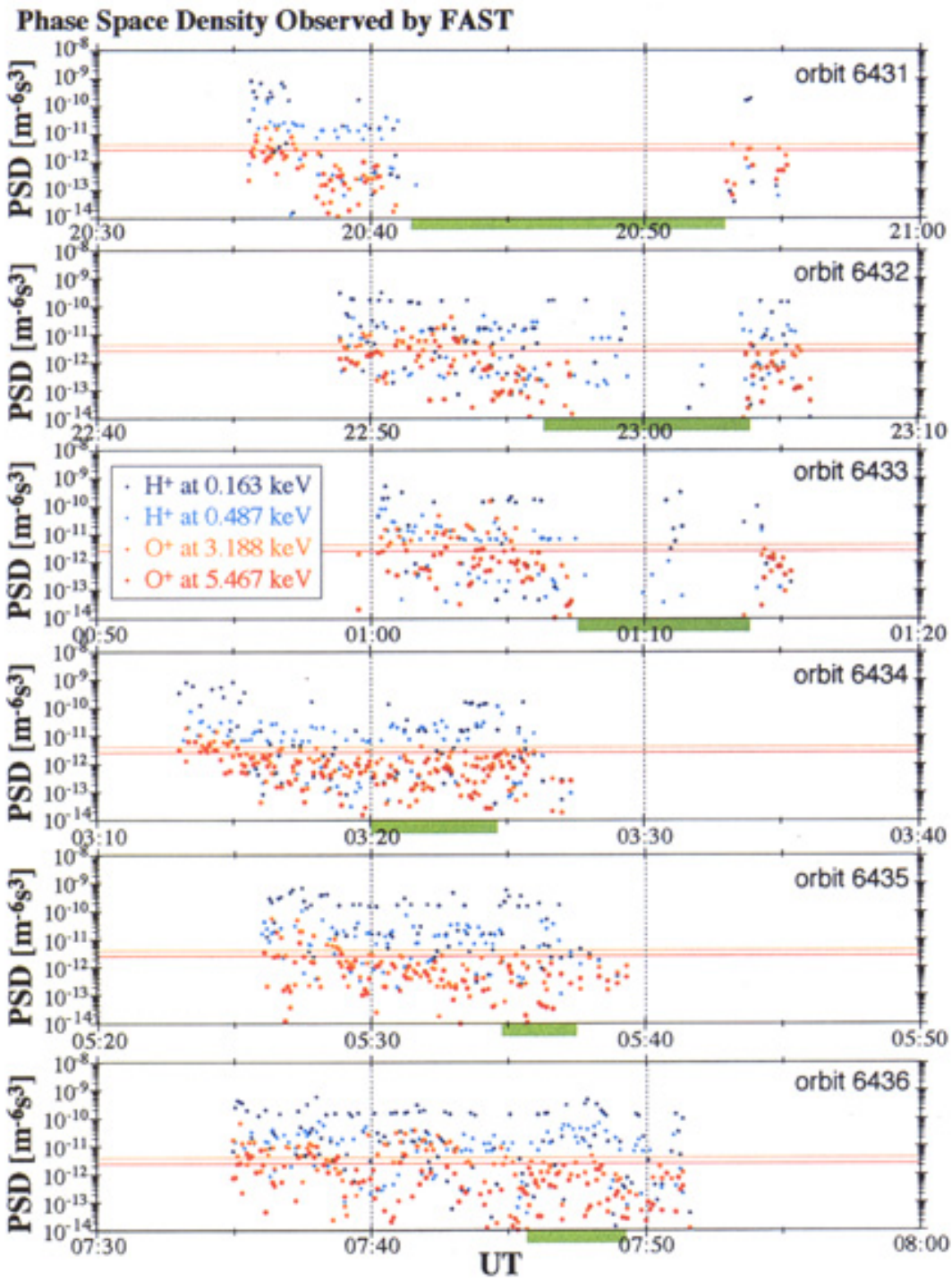

Plate 6. Phase space density (PSD) of O^+ and H^+ observed by FAST at the same energies as those shown in Plate 5. The different color marks represent the same ion species and energy as in Plate 5. Though no error bar is shown to avoid intricacy, these results can contain errors as explained in the text, and typical error levels for 0.163 keV H^+ (dark-blue), 0.487 keV H^+ (light-blue), 3.188 keV O^+ (orange), and 5.467 keV O^+ (red) correspond to ~1, ~2, ~12, and ~14 % of displayed PSD values, respectively. From the top, each panel corresponds to orbits 6431-6436. The green bar at the bottom of each panel corresponds to the time intervals when the downward He^{++} flux is enhanced or the polar cap is observed. The horizontal orange and red lines display average values of the O^+ PSD observed by Geotail at energies of 3.188 and 5.467 keV, respectively.

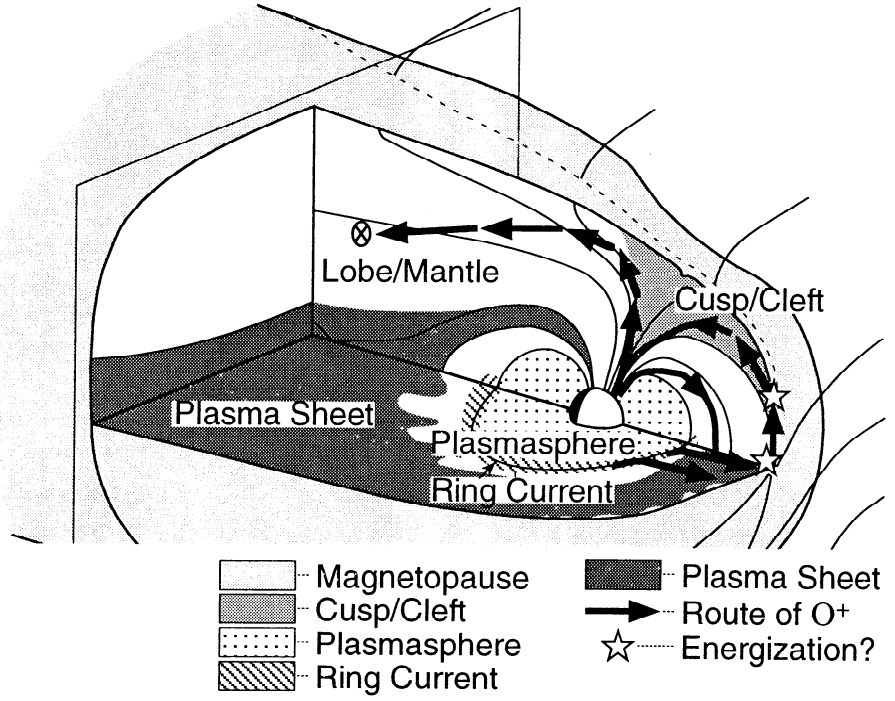

Figure 3. A three-dimensional schematic cutaway of the magnetosphere during negative IMF B_y and B_z. This figure illustrates the supply scenario of O^+ ions to the magnetotail lobe/mantle with the trapped ions in dayside magnetosphere as a source.

2. O^+ PSD in the high-energy precipitation region on closed flux tubes is comparable to that of COBs observed by Geotail.

3. In the LLBL-like regions where the magnetosheath and dayside magnetospheric plasmas are precipitating together, the PSD of precipitating O^+ is typically smaller than but sometimes comparable to that of COBs.

These results show that O^+ population in the dayside magnetosphere on closed flux tubes is adequate in quantity to supply COBs in the lobe/mantle. It is the first identification of the dayside magnetospheric plasmas as a probable source of heavy ions of terrestrial origin in the magnetotail. However, it does not deny the possibility that ionospheric polar outflows is a source of some COBs, since Geotail sometimes observes low-energy O^+ beams especially in the near-Earth regions which can be explicable with this conventional source and the extent of extra energization of these outflowing O^+ ions at high altitudes is not fully understood. The relative contribution of each probable sources of COBs needs to be investigated. Ongoing statistical studies on ion precipitation in the polar magnetosphere for different ion species will provide important information.

The O^+ PSD on the open flux tubes which is smaller than that on the closed ones suggests the importance of ion dynamics in the dayside reconnection process. Namely, the amount of O^+ originally on closed flux tubes that can remain in the magnetosphere or near the magnetopause when these flux tubes are reconnected with IMF at the dayside magnetopause will be a key issue for further discussions. In this paper, we compared PSDs at the same energies observed by Geotail in the plasma mantle and FAST on closed flux tubes. However, depending upon the ratio of energized and unenergized O^+ in the precipitation, we may also need to compare PSD at different energies for the precipitation on closed flux tubes to properly take account of the energization around the reconnection site. In order to answer these issues, a close examination of the observational information provided by multiple spacecraft, as well as the theoretical information provided by such a method as global test particle simulations in a realistic field configuration will play a crucial role.

Acknowledgments. We are grateful to the FAST PI Chuck W. Carlson, James P. McFadden, and all the ESA and TEAMS teams for the data and software used in this study. Authors especially thank Eric Dors for his extensive effort to build convenient data processing environment for FAST data at LANL. We would like to also thank all Geotail and Wind science members for their collaboration. This work was carried out under the auspices of the Research Fellowships of the Japan Society for the Promotion of Science for Young Scientists.

Janet G. Luhmann thanks Andrew W. Yau and David T. Young for their assistance in evaluating this paper.

References

Carlson, C. W., and J. P. McFadden, Design and applications of imaging plasma instruments, in *Measurement Techniques in Space Plasmas, Geophys. Monogr. Ser.*, vol. 102, edited by J. Borovsky, R. Pfaff, and D. T. Young, pp. 125-140, AGU, Washington, D. C., 1998.

Carlson, C. W., R. F. Pfaff, and J. G. Watzin, The Fast Auroral SnapshoT (FAST) mission, *Geophys. Res. Lett.*, *25*, 2013-2016, 1998.

Chappell, C. R., T. E. Moore, and J. H. Waite Jr., The ionosphere as a fully adequate source of plasma for the Earth's magnetosphere, *J. Geophys. Res.*, *92*, 5896-5910, 1987.

Chen, M. W., L. R. Lyons, and M. Schulz, Simulations of phase space distributions of storm time proton ring current, *J. Geophys. Res.*, *99*, 5745-5759, 1994.

Cowley, S. W. H., J. P. Morelli, and M. Lockwood, Dependence of convective flows and particle precipitation in the high-latitude dayside ionosphere on the X and Y components of the interplanetary magnetic field, *J. Geophys. Res.*, *96*, 5557-5564, 1991.

Curran, D. B., and C. K. Goertz, Particle distributions in a two dimensional reconnection field geometry, *J. Geophys. Res.*, *94*, 272-286, 1989.

Delcourt, D. C., J.-A. Sauvaud, O. L. Vaisberg, L. A. Avanov, J. L. Burch, and J. H. Waite Jr., Signatures of impulsive convection in the magnetospheric lobes, *Geophys. Res. Lett.*, *23*, 129-132, 1996.

Fujimoto, M., T. Mukai, A. Matsuoka, A. Nishida, T. Terasawa, K. Seki, H. Hayakawa, T. Yamamoto, S. Kokubun, and R. P. Lepping, Dayside reconnected field lines in the south-dusk near-tail flank during an IMF $B_y > 0$ dominated period, *Geophys. Res. Lett.*, *24*, 931-934, 1997.

Fuselier, S. A., D. M. Klumpar, and E. G. Shelley, Ion reflection and transmission during reconnection at the Earth's subsolar magnetopause, *Geophys. Res. Lett.*, *18*, 139-142, 1991.

Fuselier, S. A., M. Lockwood, T. G. Onsager, and W. K. Peterson, The source population for the cusp and cleft/LLBL for southward IMF, *Geophys. Res. Lett.*, *26*, 1665-1668, 1999.

Gosling, J. T., D. N. Baker, S. J. Bame, W. C. Feldman, R. D. Zwickl, and E. J. Smith, North-south and dawn-dusk plasma asymmetries in the distant tail lobes: ISEE-3, *J. Geophys. Res.*, *90*, 6354-6360, 1985.

Gosling, J. T., M. F. Thomsen, S. J. Bame, R. C. Elphic, and C. T. Russell, Cold ion beams in the low latitude boundary layer during accelerated flow events, *Geophys. Res. Lett.*, *17*, 2245-2248, 1990.

Hirahara, M., T. Mukai, T. Terasawa, S. Machida, Y. Saito, T. Yamamoto, and S. Kokubun, Cold dense ion flows with multiple components observed in the distant tail lobe by Geotail, *J. Geophys. Res.*, *101*, 7769-7784, 1996.

Hirahara, M., K. Seki, and T. Mukai, Cold dense ion flows in the distant magnetotail: The Geotail results, in *New Perspectives on the Earth's Magnetotail*, *Geophys. Monogr. Ser.*, vol. 105, edited by A. Nishida et al., pp. 45-60, AGU, Washington, D. C., 1998.

Kokubun, S., T. Yamamoto, M. H. Acuña, K. Hayashi, K. Shiokawa, and H. Kawano, The Geotail magnetic field experiment, *J. Geomagn. Geoelectr.*, *46*, 7-21, 1994.

Möbius, E., et al., The 3-D plasma distribution function analyzers with time-of-flight mass discrimination for Cluster, FAST, and Equator-S, in *Measurement Techniques in Space Plasmas: Particles*, *Geophys. Monogr. Ser.*, vol. 102, edited by J. Borovsky, R. Pfaff, and D. T. Young, pp. 243-248, AGU, Washington, D. C., 1998.

Mukai, T., M. Hirahara, S. Machida, Y. Saito, T. Terasawa, and A. Nishida, Geotail observation of cold ion streams in the medium distance magnetotail lobe in the course of a substorm, *Geophys. Res. Lett.*, *21*, 1023-1026, 1994a.

Mukai, T., S. Machida, Y. Saito, M. Hirahara, T. Terasawa, N. Kaya, T. Obara, M. Ejiri, and A. Nishida, The low energy particle (LEP) experiment onboard Geotail satellite, *J. Geomagn. Geoelectr.*, *46*, 669-692, 1994b.

Newell, P. T., and C. -I. Meng, The cusp and boundary layer: Low altitude identification and statistical local time variation, *J. Geophys. Res.*, *93*, 14,549-14,556, 1988.

Newell, P. T., and C. -I. Meng, Mapping the dayside ionosphere to the magnetosphere according to particle precipitation characteristics, *Geophys. Res. Lett.*, *19*, 609-612, 1992.

Sauvaud, J. A., Yu. I. Galperin, V. A. Gladyshev, A. K. Kuzmin, T. M. Muliarchick, and J. Crasnier, Spatial inhomogeneity of magnetosheath proton precipitation along the dayside cusp from the ARCAD experiment, *J. Geophys. Res.*, *85*, 5105-5112, 1980.

Seki, K., M. Hirahara, T. Terasawa, I. Shinohara, T. Mukai, Y. Saito, S. Machida, T. Yamamoto, and S. Kokubun, Coexistence of Earth-origin O^+ and solar wind-origin H^+/He^+ in the distant magnetotail, *Geophys. Res. Lett.*, *23*, 985-988, 1996.

Seki, K., M. Hirahara, T. Terasawa, T. Mukai, Y. Saito, S. Machida, T. Yamamoto, and S. Kokubun, Statistical properties and possible supply mechanisms of tailward cold O^+ beams in the lobe/mantle regions, *J. Geophys. Res.*, *103*, 4477-4490, 1998a.

Seki, K., T. Terasawa, M. Hirahara, and T. Mukai, Quantification of tailward cold O^+ beams in the lobe/mantle regions with Geotail data: Constraints on polar O^+ outflows, *J. Geophys. Res.*, *103*, 29,371-29,381, 1998b.

Seki, K., M. Hirahara, T. Terasawa, T. Mukai, and S. Kokubun, Properties of He^+ beams observed by Geotail in the lobe/mantle regions: Comparison with O^+ beams, *J. Geophys. Res.*, *104*, 6973-6985, 1999.

Sonnerup, B. U. Ö., Magnetic field reconnection at the magnetopause: An overview, in *Magnetic Reconnection in Space and Laboratory Plasmas*, *Geophys. Monogr. Ser.*, vol. 30, edited by E. W. Hones Jr., p. 92, AGU, Washington, D. C., 1984.

Stokholm, M., H. Balsiger, J. Geiss, H. Rosenbauer, D. T. Young, Variations of the magnetospheric ion number densities near geostationary orbit with solar activity, *Ann. Geophys.*, *7*, 69-76, 1989.

Weimer, D. R., Models of high-latitude electric potentials derived with a least error fit of spherical harmonic coefficients, *J. Geophys. Res.*, *100*, 19,595-19,607, 1995.

Weimer, D. R., A flexible, IMF dependent model of high-latitude electric potentials having "space weather" applications, *Geophys. Res. Lett.*, *23*, 2549-2552, 1996.

Woch, J., and R. Lundin, Magnetosheath plasma precipitation in the polar cusp and its control by the interplanetary magnetic field, *J. Geophys. Res.*, *97*, 1421-1430, 1992.

Yau, A. W., and M. André, Source of ion outflow in the high latitude ionosphere, *Space Sci. Rev.*, *80*, 1-25, 1997.

Young, D. T., H. Balsiger, and J. Geiss, Correlations of magnetospheric ion composition with geomagnetic and solar activity, *J. Geophys. Res.*, *87*, 9077-9096, 1982.

J. Bonnell, Space Science Laboratory, University of California Berkeley, CA 94720, USA. (jbonnell@ssl.berkeley.edu)

R. C. Elphic, K. Seki, and M. F. Thomsen, Space and Atmospheric Sciences Group (NIS-1), MS D466, Los Alamos National Laboratory, Los Alamos, NM 87545, USA. (relphic@lanl.gov, seki@lanl.gov, mthomsen@lanl.gov)

M. Hirahara, Department of Physics, College of Science, Rikkyo University, 3-34-1 Nishi-Ikebukuro, Toshima, Tokyo 171-8501, Japan. (hirahara@se.rikkyo.ac.jp)

E. J. Lund, Space Science Center, Morse Hall, University of New Hampshire, Durham, NH 03824, USA. (Eric.Lund@unh.edu)

T. Mukai, Institute of Space and Astronautical Science, 3-1-1 Yoshinodai, Sagamihara, Kanagawa 229-8510, Japan. (mukai@stp.isas.ac.jp)

K. Seki and T. Terasawa, Department of Earth and Planetary Sciences, Graduate School of Science, University of Tokyo, 7-3-1 Hongo, Bunkyo, Tokyo 113-0033, Japan. (seki@space.eps.s.u-tokyo.ac.jp; terasawa@eps.s.u-tokyo.ac.jp)

(Received August 31, 1999; revised October 19, 1999;
accepted October 22, 1999.)